Carbohydrate Polymers 92 (2013) 2095–2102

Contents lists available at SciVerse ScienceDirect

Carbohydrate Polymers

journal homepage: www.elsevier.com/locate/carbpol

Calcium alginate beads encapsulated PMMA-*g*-CS nano-particles for α-chymotrypsin immobilization

M.A. Abd El-Ghaffar*, M.S. Hashem

Polymers and Pigments Department, National Research Center, Dokki, Giza, Egypt

ARTICLE INFO

Article history:
Received 13 October 2012
Received in revised form
22 November 2012
Accepted 26 November 2012
Available online 5 December 2012

Keywords:
PMMA-*g*-CS nano-particles
Free-emulsifier emulsion polymerization
α-Chymotrypsin immobilization
PMMA-*g*-CS-CT/CA beads

ABSTRACT

Chitosan grafted with polymethyl methacrylate (PMMA-*g*-CS) was prepared *via* a free-radicals polymerization technique as a carrier for enzyme immobilization. α-Chymotrypsin (CT), as an enzyme model in this study, was immobilized onto the prepared PMMA-*g*-CS *via* covalent bonding. Calcium alginate (CA) beads were developed for encapsulating PMMA-*g*-CS-CT to produce PMMA-*g*-CS-CT/CA composite beads. Morphology and size of PMMA-*g*-CS particles were investigated by TEM and found to be in the nanoscale. The structure and surface morphology of the beads before and after immobilization process were characterized by FT-IR and SEM, respectively. Both the bound CT content and relative activity of immobilized enzyme were measured. A higher retained activity (about 97.7%) obtained for the immobilized CT at pH 9 for 24 h. The results indicated that immobilized CT maintained excellent performance even after 25 reuses and retained 75% from its original activity after 60 days of storage at 25 °C.

1. Introduction

Nowadays, nanostructure natural polymers have drawn extensive attention as carriers for enzyme immobilization technology due to their small size, high surface area, nontoxicity, excellent biocompatibility and strong adsorption ability (Chun et al., 1996; Lee et al., 2009; Li, Zhu, Zhang, Xie, & Feng, 2012; Sun, Zhang, Dong, & Shen, 2010; Sun, Qin, Gao, Li, & Jiao, 2010; Zhang et al., 2009).

Chitosan, a functional linear polysaccharide, is a naturally occurring polymer of β-(1–4)-2-amino-2-deoxy-D-glucopyranose, prepared by partial alkaline deacetylation of chitin, a main structural component of the cuticles of insects, mollusks, and crustacean. Chitosan has many significant biological and chemical properties such as biodegradability, biocompatibility, nontoxicity, and low non specific adsorption. In addition, chitosan appears economically attractive since chitin is the abundant natural polymer next to cellulose. Thus, it has been widely used in many industrial and biomedical applications including wastewater treatment, chromatographic support, enzyme immobilization, and carriers for controlled drug delivery (Abd El-Ghaffar & Hashem, 2009; Abd El-Ghaffar & Hashem, 2010; Petchthanasombat, Tiensing, & Sunintaboon, 2012).

Another type of natural polysaccharide of interest with respect to enzyme immobilization is calcium alginate (CA). CA hydrogel beads are one of the most commonly used carriers in the entrapment immobilization of biocatalyst owing to their significant advantages such as good biocompatibility, low cost, easy availability, and simplicity of preparation (Lu, Xu, Jiang, Yuan, & Wang, 2005; Morch, Donati, Strand, & Skjäk-Bræk, 2006). However, some disadvantages are often associated with this carrier, including high biomolecule leakage, low mechanical strength and large pore size (Konsoula and Liakopoulou-Kyriakides, 2006).

α-Chymotrypsin (EC 3.4.21.1), an endoprotease, is one of the three principal protein-degrading or proteolytic enzymes in the digestive system, the other two being pepsin and trypsin. The three enzymes were among the first to be isolated in crystalline form. During the process of digestion, these enzymes, each of which is particularly effective in severing links between particular types of amino acids, collaborate to break down dietary proteins to their components, *i.e.*, peptides and amino acids, which can be readily absorbed by the intestinal lining. In the laboratory studies α-chymotrypsin is most efficient in cleaving bonds of protein chains at the C-terminal position with aromatic amino acids (tryptophan, tyrosine, or phenylalanine) and yielding the mixture of peptides of different molecular sizes or free amino acids (Altun & Cetinus, 2007; Ju et al., 2012).

Therefore the goal of this study is to encapsulate α-chymotrypsin within CA beads by conjugating the enzyme with the

* Corresponding author. Tel.: +20 122 7901129; fax: +20 2 33355146.
E-mail address: mghaffar50@yahoo.com (M.A. Abd El-Ghaffar).

0144-8617/$ – see front matter © 2012 Elsevier Ltd. All rights reserved.
http://dx.doi.org/10.1016/j.carbpol.2012.11.084

amino groups of PMMA-*g*-CS nano-particles and then encapsulated them within CA beads.

2. Experimental

2.1. Materials

Chitosan (CS) (degree of deacetylation: 85%, Brookfield viscosity: 20,000 cps, low molecular weight), methyl methacrylate (MMA) and bovine serum albumin (BSA) were obtained from Aldrich. α-Chymotrypsin (CT) (EC 3.4.21.1 from bovine pancreas) and sodium alginate (SA) (low viscosity: 250 cps, MW: 12–80 kDa) were purchased from Fluka. N-acetyl-L-tyrosine ethyl ester (ATEE) and N-acetyl-L-tyrosine were obtained from Molekula. Folin reagent, calcium chloride ($CaCl_2$) and ammonium per sulfate (APS) were purchased from Merck. Double distilled water (DDW) was used in all experiments. Other chemicals and reagents employed were of analytical grade and were used without any further purification.

2.2. Methods

2.2.1. Preparation of PMMA-g-CS nano-particles

For the synthesis of the PMMA-*g*-CS nano-particles, a free-radicals polymerization technique was employed using APS as an initiator. The polymerization was carried out in a three necked flask (100 ml) fitted with a condenser and a thermometer. The system also had a nitrogen inlet and was stirred with a magnetic stirrer. Before subjected to polymerization, CS (1 g) was dissolved in 1% acetic acid aqueous solution and DDW (50 ml) were added into the reaction vessel and heated to 65 °C while flushing nitrogen through the solution. Then specific amount of MMA and APS (0.15 g) were added and the reaction ingredients were stirred vigorously at 65 °C for 4 h. The prepared stable emulsion was transferred to Petri dish till air-dried latex was formed. The dialysis of PMMA-*g*-CS nano-particles latex against ethanol and DDW was carried out for 7 days to remove unreacted vinyl monomer. Finally, the nano-particles were resuspended in 50 ml DDW and stored at room temperature for further uses.

2.2.2. Immobilization of α-chymotrypsin

The dried PMMA-*g*-CS nano-particles (100 mg) were immersed into 5 ml of 1 mg/ml of CT solution in sodium borate buffer (0.1 M, pH 9.0). The immobilization reaction was allowed to proceed for 24 h at 25 °C. After the immobilization was completed, the appropriate amount of SA was added into the above mixture and was further stirred at 1000 rpm for 4 h to ensure homogeneity of the mixture. The mixture was dropped into a gently stirred $CaCl_2$ solution through a fine stainless steel needle. The distance between the edge of the needle and the surface of the calcium solution was 15 cm. PMMA-*g*-CS-CT/CA beads were formed instantaneously and were left in the gelling medium for 15 min, then separated from the solution through a stainless steel grid. The obtained PMMA-*g*-CS/CA-CT beads were rinsed with distilled water for three times to remove unreacted $CaCl_2$ on surface and subsequently dried at room temperature for 15 min before used for further investigations.

2.3. Tests

2.3.1. Determination of monomer conversion and solid content

The percentage of monomer conversion and solid content was determined from gravimetric analysis. About 2 g of PMMA-*g*-CS nano-particle latex prepared was taken into a pre-weighed Petri dish. The air-dried latex was further dried in a vacuum oven at 70 °C. The monomer conversion and solid content were calculated from the following equations:

$$\%\,\text{Conversion} = \frac{\text{weight of dried latex} - \text{weight of CS}}{\text{weight of monomer feed}} \times 100$$

$$\%\,\text{Solid content} = \frac{\text{weight of dried latex}}{\text{weight of latex}} \times 100$$

2.3.2. Determination of grafting efficiency and percentage of PMMA

The dried PMMA-*g*-CS nano-particles were taken into pre-weighed dialysis bag and then dialysis reaction against dichloromethane was carried out for 2 days to remove the homo-PMMA. The grafting efficiency and grafting percentage were calculated from as follows:

$$\text{Grafting efficiency} = \frac{\text{weight of grafted PMMA}}{\text{weight of the total polymerized MMA}} \times 100$$

$$\%\,\text{Grafting percentage} = \frac{\text{weight of grafted PMMA}}{\text{weight of CS used}} \times 100$$

2.3.3. Determination of immobilized α-chymotrypsin content

α-Chymotrypsin content in the PMMA-*g*-CS/CA composite beads was determined with the help of the Lowry method (Lowry, Rosebrough, Farr, & Randall, 1951) by using BSA as the standard. The quantity of entrapped CT was calculated by subtracting the enzyme recovered in the combined washings of the α-chymotrypsin-polymer network from the enzyme used for immobilization.

2.3.4. α-Chymotrypsin activity assay

The activities of free and immobilized α-chymotrypsin were determined using the method of Schwert and Takenaka (Schwert & Takenaka, 1955), Garrel and Cuchillo (Garrel & Cuchillo, 1985). For the measurement of CT activity, ATEE was used: the change in absorbance at 237 nm was followed in a reaction mixture (3 ml) containing 40 mM Tris/HCl (pH 8) and 0.5 mM ATEE. The reactions were initiated by 50 μl of 0.15 mg/ml enzyme.

One unit of enzyme activity was defined as the amount of enzyme that catalyzes the hydrolysis of 1 μM of ATEE per min at pH 8.0 and at 25 °C.

2.3.5. Properties of free and immobilized α-chymotrypsin

2.3.5.1. Optimum pH. The effect of pH on the activity of free and immobilized α-chymotrypsin was assayed in the acetate buffer (0.1 M) in the pH range 3.0–6.0 and in the phosphate buffer (0.1 M) in the pH range 7.0–11.0 by using the abovementioned standard activity assay procedure.

2.3.5.2. pH stability. The pH stabilities of free and immobilized α-chymotrypsin were compared in the acetate and phosphate buffers (0.1 M) between pH 3.0 and 11. Free and immobilized enzymes were incubated at these buffer solutions for 1 h. Both forms of α-chymotrypsin were assayed using the standard assay conditions.

2.3.5.3. Optimum temperature. The effect of temperature on the activities of both forms of α-chymotrypsin was studied between 30 and 90 °C and assayed under standard assay conditions.

2.3.5.4. Thermal stability. The thermal stability of the free and immobilized α-chymotrypsin was evaluated by measuring the residual activity of α-chymotrypsin exposed to various temperatures between 30 and 90 °C, in phosphate buffer (0.1 M, pH 9.0), for 15 min. The remaining activities were expressed as relative to the original activities assayed at 25 °C.

2.3.5.5. Storage stability and reusability. The immobilized α-chymotrypsin was stored in a dry state at 25 °C for 60 days. Its activity was measured at frequent intervals. The immobilized α-chymotrypsin was repeatedly used in the catalytic reaction of ATEE, for reusability evaluation, under standard assay conditions. After each activity assay the samples were washed with the buffer and stored until the next assay.

The results of pH, temperature, reusability and storage stability of free and immobilized α-chymotrypsin were presented in a normalized form, with the highest value of each set being assigned the value of 100% activity.

2.4. Characterization

FT-IR spectra were recorded on a FT-IR spectrophotometer (Nicolet 670, range from 4000 to 400 cm^{-1}, USA) using KBr pellets. Transmission electron microscopy (TEM) was carried out using a JEM-1230 (JEOL, Japan) operating at 60 kV. Drops of the emulsion solutions were deposited on carbon coated copper grids and dried at room temperature. Surface morphology was visualized by scanning electron microscopy (SEM) (JXA-840A Electron probe microanalyzer, JEOL, Japan) using an accelerating voltage of 30 kV after coating with gold film using S150A Sputter Coater (Edwards, England). The enzyme content and the activity of free and immobilized α-chymotrypsin were measured using double-beam Spectrometer (Shimadzu UV-2401 PC, Japan).

3. Results and discussion

Chitosan is currently at the focus of increasing scientific and economic interest as an attracting biopolymer for uses in immobilization of negatively charged biomacromolecules *via* its amino groups. The modification of CS with synthetic polymers by emulsion polymerization was reported in several researches (Elizalde-Peña et al., 2007; Spagnol et al., 2012; Trpathi, Goyal, Kumar, & Gupta, 2012).

3.1. Synthesis of PMMA-g-CS nano-particles

PMMA-*g*-CS nano-particles were prepared *via* the free-radical polymerization using APS as an initiator. The nucleation and growth of nano-particles occurred as follows. The amphiphilic grafted copolymers consisting of hydrophilic CS backbone and the hydrophobic PMMA side chains were first formed and then spontaneously self-assembled to nano-particles in an aqueous medium. The presence of amino groups of CS could subsequently enhanced polymerization of the MMA monomer and resulted in higher monomer conversion percentages. The CS amino groups made both CS and APS act as co-initiators and enhanced formation of the more of free radicals (Inphonlek, Pimpha, & Sunintaboon, 2010). The proposed reaction mechanism between MMA and CS is summarized in Fig. 1(a).

The effect of the polymerization reaction parameters (*e.g.*, polymerization time and the amount of MMA added) affecting the monomer conversion, solid content, grafting efficiency and grafting percentage was studied.

3.1.1. Polymerization parameters

3.1.1.1. Effect of polymerization time. Table 1 shows the variation of MMA conversion and solid content of PMMA upon varying the polymerization time. It can be seen that when the polymerization time increased from 2 to 4 h, the conversions and solid contents also increased from 60% to 98%, and 3.3% to 4.7%, respectively. However, at the reaction time of 5 h, the precipitation of latex product apparently took place, indicating that CS on the shell could not provide sufficient colloidal stability to the particles. It can be summarized that 4 h polymerization time gives the highest conversion and stable emulsion particles latex (Petchthanasombat et al., 2012).

Table 1
Effect of polymerization time on MMA conversion and solid content.

Polymerization time	Solid content (%)	Conversion (%)
2	3.3	60.6
3	3.9	77.9
4	4.7	98.7
5	Latex precipitated	Latex precipitated

3.1.1.2. Effect of concentration of MMA. Table 2 shows that the variation in MMA concentration results in the extent of monomer conversion, grafting percentage as well as solid content. It was observed that, increasing MMA concentration up to 0.75 mol is accompanied by an increase in the above-mentioned properties. At 1 mol of MMA the precipitation of latex product apparently took place. From these results, it can be concluded that the optimum amount of MMA is 0.75 mol and the prepared PMMA-*g*-CS nanoparticles with 0.75 mol was used in the immobilization reaction and all other investigations and tests.

3.2. Characterization of nanoparticles and beads

3.2.1. FT-IR spectroscopy

The prepared graft copolymers and beads were characterized by FT-IR spectra. From the CS spectrum (Fig. 2(a)) distinctive absorption bands at 3500–3200 cm^{-1} (O—H stretching and N—H stretching), 2881 cm^{-1} (C—H stretching), 1658 (amide I), 1587 (—NH_2 binding) and 1380 (amide III) can be found. The absorption bands at 1157 cm^{-1} (anti-symmetric stretching of the C—O—C bridge), 1081 and 1033 cm^{-1} (skeletal vibration involving the C—O stretching) are characteristic of its saccharide structure. The absorbance at 2952 cm^{-1} (vs. CH_2), was stronger in the copolymer. The new band appears at 1731 cm^{-1}, which corresponds to C=O of the ester group stretching vibration of MMA, was observed in the grafted CS spectrum (Fig. 2(b–d)). This is a typical absorption of MMA, which confirms that MMA has been successfully grafted onto the CS backbone. The new bands presenting in the IR spectrum (Fig. 2(e)) at 1623 and 1455 cm^{-1} are assigned to asymmetric and symmetric stretching peaks of carboxylate salt groups which attributed to the presence of CA.

The IR spectrum of α-chymotrypsin (Figs. 2(g)) contains characteristic absorption bands peaked at about 1644 (amide I), 1536 (amide II), 1236 (amide III), 590 cm^{-1} (amide V), as well as bands peaked at about 2963 (C—H stretching vibrations) and 3295 cm^{-1} (N—H stretching vibrations). New bands appear at 1390, 1243 (C—N—H vibration from conjugation of α-chymotrypsin with CS), 1194 (CH_2—NH_2 from α-chymotrypsin), 989, and 841 cm^{-1} (Fig. 2(f)). The band at 3447 becomes broad due to the stretching vibration of the amino (from α-chymotrypsin), amide (CO—NH from conjugation of α-chymotrypsin with CS) and hydroxyl groups (from α-chymotrypsin and CS). This confirms that α-chymotrypsin is strongly covalently bound to PMMA-*g*-CS nano-particles encapsulated in CA beads. These results are in accordance with the previous results (Boonsongrit, Mueller, & Mitrevej, 2008; Shantha & Harding, 2002; Zhang, Yuan, Shen, & Lin, 2003).

3.2.2. Nanoparticles and beads morphology

The TEM graphs of PMMA-*g*-CS nano-particles are shown in Fig. 3(a–c). By investigating the TEM photographs, the average size of the nano-particles was 75 nm, 95 nm and 100 nm for 0.25, 0.5 and 0.75 mol of MMA respectively. As clearly seen here, the dispersion of PMMA-*g*-CS nano-particles was well spherical-like in shape.

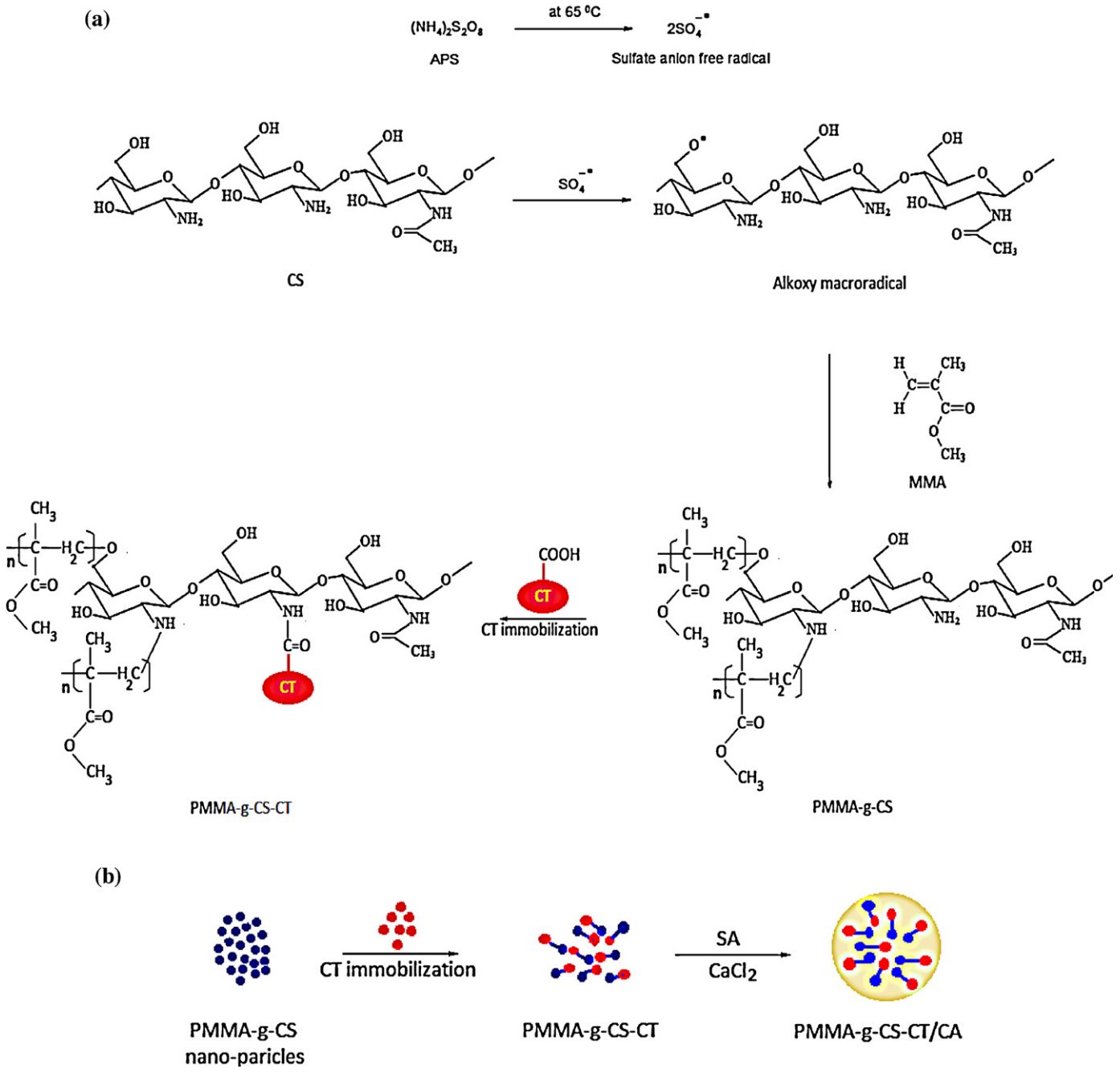

Fig. 1. Schematic illustration of (a) grafting reaction mechanism of PMMA on chitosan and the immobilization of CT onto PMMA-g-CS, and (b) encapsulation of PMMA-g-CS-CT within CA beads.

The SEM micrographs of PMMA-*g*-CS/CA and PMMA-*g*-CS-CT/CA beads are shown in Fig. 3. It is observed that the composite formed by embedded the PMMA-*g*-CS nano-particles within the CA bead was in a very uniform spherical shape (Fig. 3(d)). Focusing on the surface and the interior part of the bead, it is noticed that both of them have spongy structures (Fig. 3(e) and (f)). After CT immobilization by encapsulation the bead still has a spherical shape (Fig. 3(g)). The presence of CT particles was seen in the exterior (Fig. 3(h)) and the interior (Fig. 3(i)) of the PMMA-*g*-CS-CT/CA bead. The spongy and porosity structure of PMMA-*g*-CS/CA composite facilitate the penetration of substrate and the product of hydrolysis by immobilized CT. Different concentrations of CT were

Table 2
Effect of MMA amount on solid content, MMA conversion, grafting efficiency and grafting percentage.

MMA amount (mol)	Solid content (%)	Conversion (%)	Grafting efficiency (%)	Grafting percentage (%)
0.25	1.93	74	55	61
0.50	3.15	86	72	78
0.75	4.68	98	95	90
1	Latex precipitated	Latex precipitated	Latex precipitated	Latex precipitated

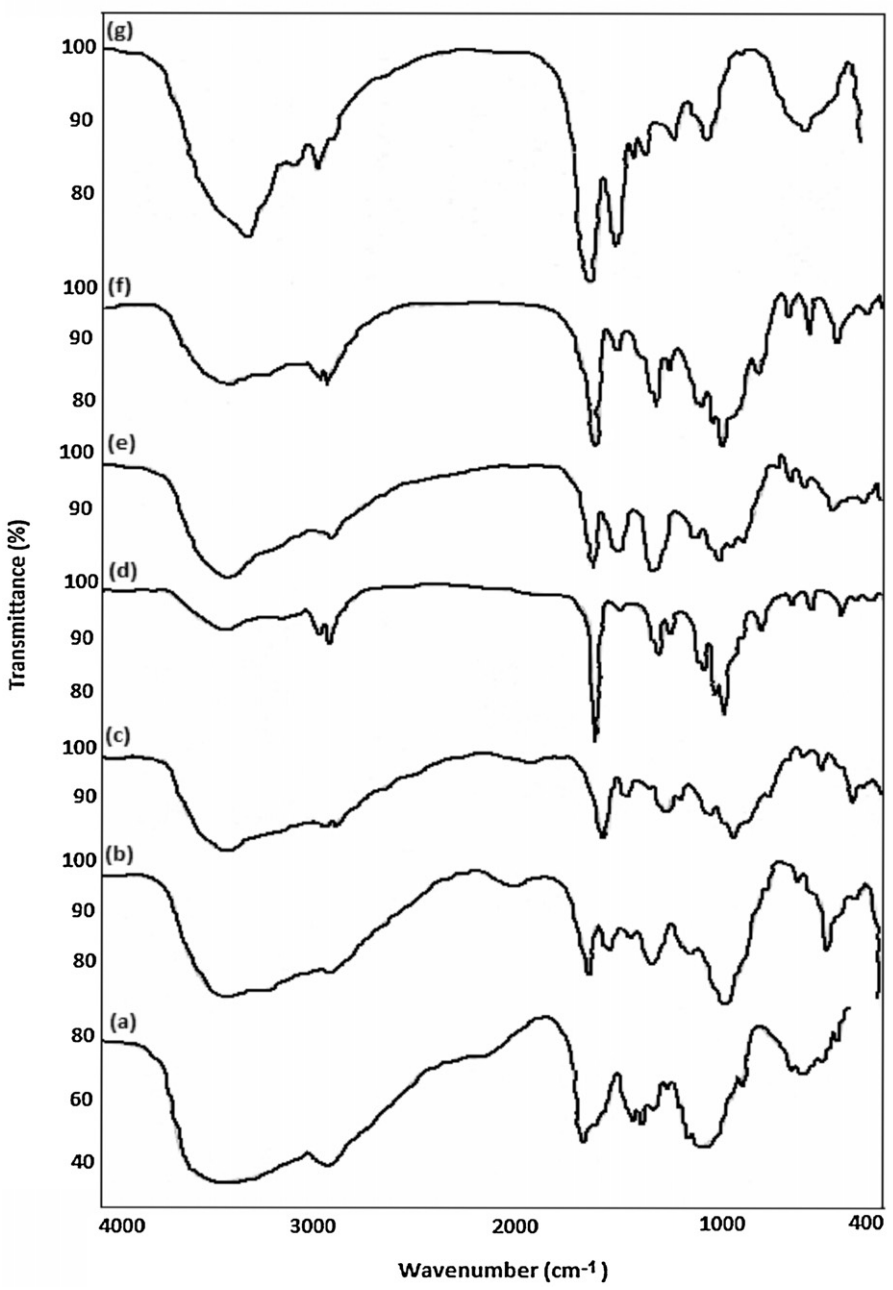

Fig. 2. FT-IR of (a) chitosan, (b) PMMA-*g*-CS (0.25 mol), (c) PMMA-*g*-CS (0.5 mol), (d) PMMA-*g*-CS (0.75 mol), (e) PMMA-*g*-CS/CA, (f) PMMA-*g*-CS-CT/CA, and (g) CT.

used in the immobilization reaction and the presence of their particles is proved by investigating the morphology of the inner beads as show in Fig. 3(j–l).

3.3. α-Chymotrypsin immobilization

A direct immobilization of carboxyl-bearing enzyme (CT) was performed by means of coupling to the amino groups of PMMA-*g*-CS nano-particles at static conditions. The dried PMMA-*g*-CS nano-particles were immersed into 5 ml solution containing different ratios of CT in sodium borate buffer (0.1 M, pH 9.4) at 25 °C. After specific time intervals of the immobilization reaction, the appropriate amount of SA was added into the above mixture and then the mixture was dropped into a gently stirred $CaCl_2$ solution. The formation of CA beads containing PMMA-*g*-CS-CT protected the activity of the enzyme during the subjected tests after immobilization process. The morphology of these beads, as discussed in Section 3.2.2, allowed the catalytic process between CT and its substrate without high leaching from the PMMA-*g*-CS or high loss of its activity. Various concentrations of SA (0.5–5%) were used during the formation of the PMMA-*g*-CS-CT/CA beads. We found that when the SA concentration was higher than 3 wt%, the solution became extremely viscous. Furthermore, we found that the use of a low SA concentration (0.5% and 1%) did not produce any beads. While, at 2% of SA the weak and very rapid broken beads were formed. The optimum concentration of SA to form uniform and strong beads was 3%.

The proposed reaction mechanism of CT immobilization onto PMMA-*g*-CS nano-particles and their encapsulation in CA beads are summarized in Fig. 1(a) and (b).

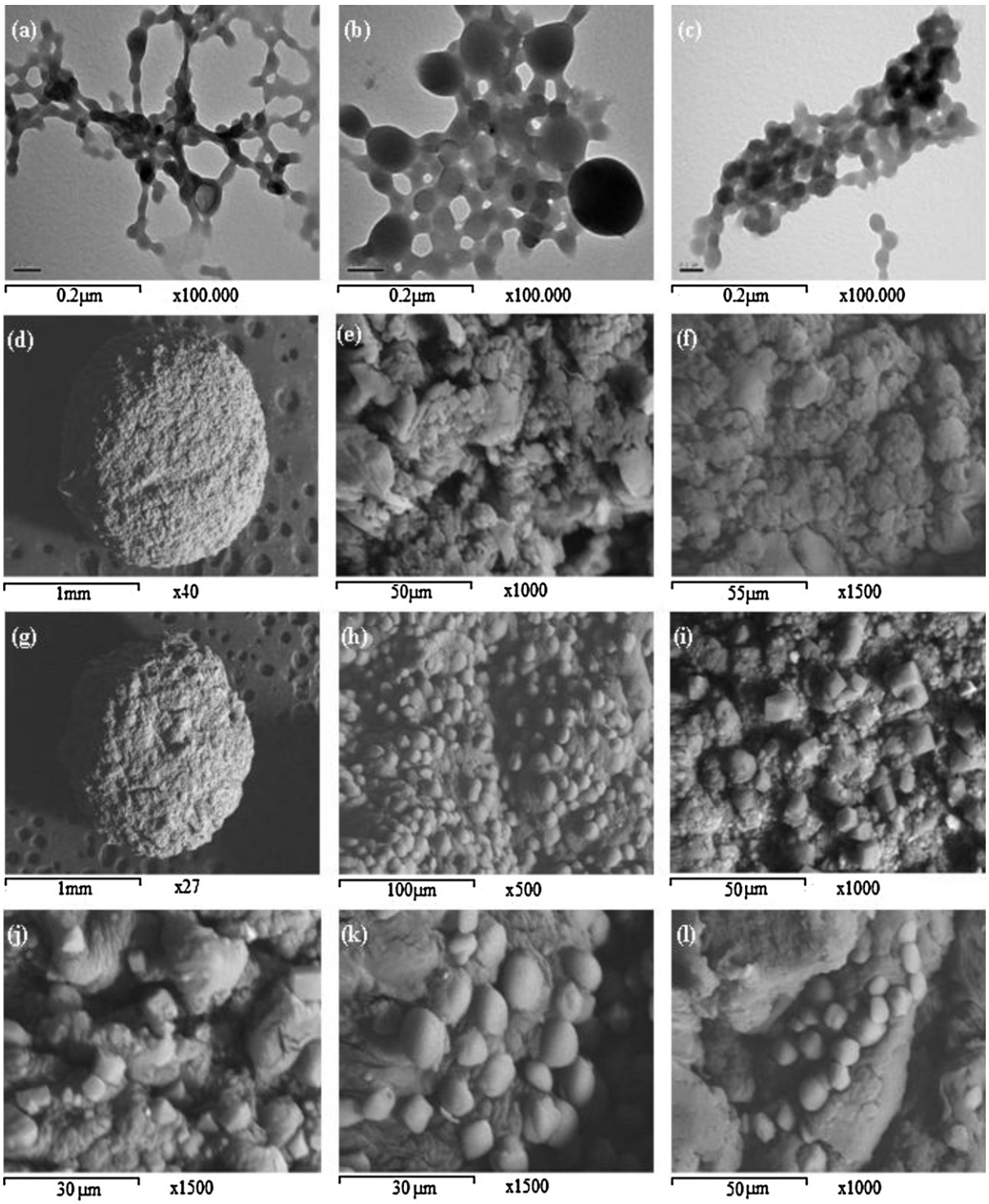

Fig. 3. TEM of (a) PMMA-*g*-CS (0.25 mol of MMA), (b) PMMA-*g*-CS (0.5 mol of MMA), and (c) PMMA-*g*-CS (0.75 mol of MMA) and SEM of (d) PMMA-*g*-CS/CA bead, (e) PMMA-*g*-CS/CA bead surface, (f) PMMA-*g*-CS/CA interior bead, (g) PMMA-*g*-CS-CT/CA bead, (h) PMMA-*g*-CS-CT/CA bead surface, (i) PMMA-*g*-CS-CT/CA interior bead, (j) PMMA-*g*-CS-CT/CA (1 mg CT) interior bead, (k) PMMA-*g*-CS-CT/CA (5 mg CT) interior bead, and (l) PMMA-*g*-CS-CT/CA (10 mg CT) interior bead.

3.3.1. Parameters affecting α-chymotrypsin immobilization

3.3.1.1. Effect of α-chymotrypsin concentration. The amounts and percentages of bound CT to PMMA-*g*-CS are shown in (Table 3). It was observed that the amount of bound CT and the retained activity were increased with increasing the CT ratio from 1 to 5 mg. However, at 10 mg of CT the retained activity was decreased, while the amount of bound CT was still high. This behavior can be attributed to the steric hindrance between immobilized CT molecules. In addition, the interior morphology of PMMA-*g*-CS-CT/CA bead (Fig. 3(l)) was very condensing which did not allow the easy penetration of the substrate during the catalytic process.

3.3.1.2. Effect of immobilization time. The effect of immobilization time was investigated. Immobilization times were selected as 4, 12 and 24 h. By increasing the time of the immobilization reaction, the amount of immobilized CT and its retained activity were

Table 3
Effect of immobilization time and CT concentration on immobilization process.

Immobilization time			CT concentration		
Time (h)	Bound CT (%)	Retained activity (%)	Concentration (mg)	Bound CT (%)	Retained activity (%)
4	47.7	65.1	1	96.7	79.1
12	79.1	87.8	5	99.5	97.7
24	99.3	97.5	10	90.8	31.6

increased. Optimum immobilization time was 24 h at which the retained activity of immobilized CT was 97.5% from its original activity (Table 3).

3.3.2. *Parameters affecting α-chymotrypsin activity*

The activities of free and immobilized CT onto PMMA-*g*-CS/CA were calculated by measuring the absorbance of the librated N-acetyl-L-tyrosine at (237 nm), taking into account that the retained activities of the immobilized CT would be the initial activities (relative activity 100%) of them in the subsequent experiments. Effect of pH values and temperatures, as well as storage stabilities, and reusability were examined.

3.3.2.1. Effect of pH. When immobilized to materials, the pH and thermal activity profiles of an enzyme can be altered (Dwevedi & Kayastha, 2009; Dwevedi, Singh, Singh, Srivastava, & Kayastha, 2009; Pan et al., 2009; Sun, Zhang, et al., 2010; Sun, Qin, et al., 2010). The effect of pH on CT activity has been investigated by varying the pH of buffer from 3.0 to 11.0. No changes in the optimum pH (pH 9.0) of free and immobilized CT onto PMMA-*g*-CS/CA as observed in Fig. 4(a). This behavior may be due to the immobilization reaction through the free carboxyl group of the enzyme. Accordingly the medium became alkaline according to the free and unreacted amino groups of the CT and the PMMA-*g*-CS polymer carrier, respectively (Chengyou, Kai, Anthony, & Deshan, 2006). The retained activity of free CT at pH 3–6 was very low (1–25%), while the retained activity of the immobilized one was 55–75%. This result indicated that the CT, once immobilized on PMMA-*g*-CS/CA, increase its acid-resisting capacity. This is due to the immobilized enzyme is less sensitive to pH changes than that of free CT (Talbert & Hotchkiss, 2012).

3.3.2.2. Effect of temperature. In general, activity of the immobilized enzyme, especially in a covalently bound system, is more thermal resistance than that of the soluble one (Hong et al., 2006). In order to determine the effect of temperature on the free and immobilized CT, their catalytic activities were measured over a range of temperatures from 30 to 100 °C. As seen in Fig. 4(b), with increase in temperature the percentage of decrease in the catalytic efficiency of free CT is reasonable but immobilized enzyme shows increasing in catalytic activity. At 100 °C, the immobilized CT retained 85% of its original activity whereas the free urease lost all at 75 °C. The enhancement of thermal stability of immobilized CT is attributed to covalent bonding between amino groups of PMMA-*g*-CS and CT, which may restrict the conformational change of CT through heating. The improved thermal stability of enzyme was attributed to the encapsulation of the PMMA-*g*-CS-CT within CA beads. The presence of special water structuring properties of hydroxyl groups on beads prevents the denaturation of CT (Sahoo, Sahu, & Pramanik, 2011; Tortajada, Ramon, Beltrand, & Amoros, 2005).

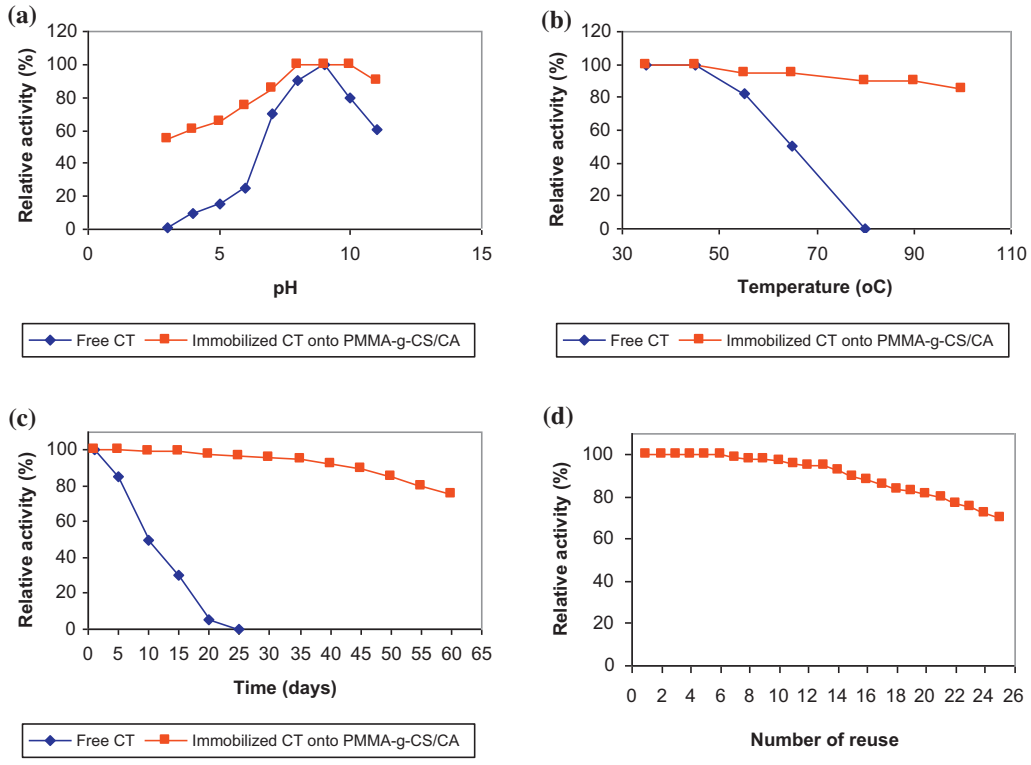

Fig. 4. Parameters affecting CT activity: (a) pH and (b) temperature, (c) storage stability of free and immobilized CT onto PMMA-*g*-CS/CA beads at 25 °C and (d) reusability of immobilized CT onto PMMA-*g*-CS/CA beads in repeated hydrolysis.

3.3.2.3. Storage stability. The covalent immobilization definitely held the immobilized enzyme in a stable position in comparison to the free counterpart (Hong et al., 2007). Free and immobilized CT onto PMMA-*g*-CS/CA was stored in dry state at 25 °C, and the catalytic activity measurements were carried out for 60 days. The free CT lost all of its activity within 25 days, whereas the immobilized one lost only about 3% of their activities during the same period as shown in Fig. 4(c). The immobilized CT preserved 75% from its original activity after 60 days of storage at 25 °C. The experiment revealed that storage stability of the bound CT was improved in comparison to free CT.

3.3.2.4. Reusability. For any applications based on immobilized enzymes, the feasibility of regeneration of the enzyme activity and consequent reuse of the biocatalyst are beneficial for its industrial productions (Zhang, Wang, Zhou, He, & Yu, 2012). The operational stability of immobilized CT onto PMMA-*g*-CS/CA was obtained by running measurements in the same day of immobilization process. Between each subsequent measurement the polymeric carrier washed with phosphate buffer solution and stored for 10 min. After 13 cycles the immobilized CT retained 95% of its original activity, 30% loss of its original activity was observed after 25 times of reuse (Fig. 4(d)). Therefore, the use of immobilized CT would lead to the continuous hydrolysis without much loss of the activities. But free CT cannot be reused and recycled for next subsequent catalytic experiment.

4. Conclusions

It is obvious from the obtained results that the developed PMMA-*g*-CS/CA bead was a suitable support polymer for enzyme immobilization. CT immobilization onto PMMA-*g*-CS was firstly achieved *via* covalent attachment and then the PMMA-*g*-CS-CT nano particles were encapsulated within CA beads. The immobilized CT has a good stability in a wide range of pH and temperature over free one. Also, the immobilized CT can be used for continuous catalytic reaction without losing a lot of its activity, on contrary to the free enzyme which cannot be recycled.

References

Abd El-Ghaffar, M., & Hashem, M. (2009). Immobilization of α-amylase onto chitosan and its amino acid condensation adducts. *Journal of Applied Polymer Science*, *112*, 805–814.

Abd El-Ghaffar, M., & Hashem, M. (2010). Chitosan and its amino acids condensation adducts as reactive natural polymer supports for cellulase immobilization. *Carbohydrate Polymers*, *81*, 507–516.

Altun, G., & Cetinus, S. (2007). Immobilization of pepsin on chitosan beads. *Food Chemistry*, *100*, 964–971.

Boonsongrit, Y., Mueller, B., & Mitrevej, A. (2008). Characterization of drug–chitosan interaction by ^{1}H NMR, FTIR and isothermal titration calorimetry. *European Journal of Pharmaceutics and Biopharmaceutics*, *69*, 388–395.

Chengyou, K., Kai, K., Anthony, Y., & Deshan, L. (2006). The immobilization of trypsin on soap-free P(MMA-EA-AA) latex particles. *Materials Science and Engineering C*, *26*, 664–669.

Chun, K., Kwon, I., Kim, Y., La, S., Sohn, Y., & Jeong, S. (1996). Preparation of sodium alginate microspheres containing hydrophilic β-lactam antibiotics. *Archives of Pharmacal Research*, *19*, 106–116.

Dwevedi, A., & Kayastha, A. (2009). Optimal immobilization of β-galactosidase from Pea (*Ps*BGAL) onto Sephadex and chitosan beads using response surface methodology and its applications. *Bioresource Technology*, *100*, 2667–2675.

Dwevedi, A., Singh, A., Singh, D., Srivastava, O., & Kayastha, A. (2009). Lactose nano-probe optimized using response surface methodology. *Biosensors and Bioelectronics*, *25*, 784–790.

Elizalde-Peña, E., Flores-Ramirez, N., Luna-Barcenas, G., Vásquez-García, S., Arámbula-Villa, G., García-Gaitán, B., et al. (2007). Synthesis and characterization of chitosan-g-glycidyl methacrylate with methyl methacrylate. *European Polymer Journal*, *43*, 3963–3969.

Garrel, J., & Cuchillo, C. (1985). Different kinetic patterns in the alpha-chymotrypsin-catalysed hydrolysis of synthetic ester substrates. *FEBS Letters*, *190*, 329–332.

Hong, J., Gong, P., Yu, J., Xu, D., Sun, H., & Yao, S. (2006). Conjugation of α-chymotrypsin on a polymeric hydrophilic nanolayer covering magnetic nanoparticles. *Journal of Molecular Catalysis B: Enzymatic*, *42*, 99–105.

Hong, J., Xu, D., Gong, P., Sun, H., Dong, L., & Yao, S. (2007). Covalent binding of α-chymotrypsin on the magnetic nanogels covered by amino groups. *Journal of Molecular Catalysis B: Enzymatic*, *45*, 84–90.

Inphonlek, S., Pimpha, N., & Sunintaboon, P. (2010). Synthesis of poly(methyl methacrylate) core/chitosan-mixed-polyethyleneimine shell nanoparticles and their antibacterial property. *Colloids and Surfaces B: Biointerfaces*, *77*, 219–226.

Ju, H., Kuo, C., Too, J., Huang, H., Twu, Y., Chang, C., et al. (2012). Optimal covalent immobilization of α-chymotrypsin on Fe_3O_4–chitosan nanoparticles. *Journal of Molecular Catalysis B: Enzymatic*, *78*, 9–15.

Konsoula, Z., & Liakopoulou-Kyriakides, M. (2006). Starch hydrolysis by the action of an entrapped in alginate capsules α-amylase from *Bacillus subtilis*. *Process Biochemisty*, *41*, 343–349.

Lee, D., Ponvel, K., Kim, M., Hwang, S., Ahn, I., & Lee, C. (2009). Immobilization of lipase on hydrophobic nano-sized magnetite particles. *Journal of Molecular Catalysis B: Enzymatic*, *57*, 62–66.

Li, S., Zhu, X., Zhang, W., Xie, G., & Feng, W. (2012). Hydrogen peroxide biosensor based on gold nanoparticles/thionine/gold nanoparticles/multi-walled carbon nanotubes–chitosans composite film-modified electrode. *Applied Surface Science*, *258*, 2802–2807.

Lowry, O., Rosebrough, N., Farr, A., & Randall, R. (1951). Protein measurement with the Folin phenol reagent. *Journal of Biological Chemistry*, *193*, 265–275.

Lu, Y., Xu, S., Jiang, Z., Yuan, W., & Wang, T. (2005). Diffusion of nicotinamide adenine dinuncleotide in calcium alginate hydrogel beads doped with carbon and silica nanotubes. *Journal of Chemical and Engineering Data*, *50*, 1319–1323.

Morch, Y., Donati, I., Strand, B., & Skjäk-Bræk, G. (2006). Effect of Ca^{2+}, Ba^{2+} and Sr^{2+} on alginate microbeads. *Biomacromolecules*, *7*, 1471–1480.

Pan, C., Hu, B., Li, W., Sun, Y., Ye, H., & Zeng, X. (2009). Novel and efficient method for immobilization and stabilization of β-D-galactosidase by covalent attachment onto magnetic Fe_3O_4–chitosan nanoparticles. *Journal of Molecular Catalysis B: Enzymatic*, *61*, 208–215.

Petchthanasombat, C., Tiensing, T., & Sunintaboon, P. (2012). Synthesis of zinc oxide-encapsulated poly(methyl methacrylate)–chitosan core–shell hybrid particles and their electrochemical property. *Journal of Colloid and Interface Science*, *369*, 52–57.

Sahoo, B., Sahu, S., & Pramanik, P. (2011). A novel method for the immobilization of urease on phosphonate grafted iron oxide nanoparticle. *Journal of Molecular Catalysis B: Enzymatic*, *69*, 95–102.

Schwert, G., & Takenaka, Y. (1955). A spectrophotometric determination of trypsin and chymotrypsin. *Biochimica et Biophysica Acta*, *16*, 570–575.

Shantha, K., & Harding, D. (2002). Synthesis and characterization of chemically modified chitosan microspheres. *Carbohydrate Polymers*, *48*, 247–253.

Spagnol, C., Rodrigues, F., Pereira, A., Fajardo, A., Rubira, A., & Muniza, E. (2012). Superabsorbent hydrogel composite made of cellulose nanofibrils and chitosan-graft-poly(acrylic acid). *Carbohydrate Polymers*, *87*, 2038–2045.

Sun, S., Zhang, Y., Dong, L., & Shen, S. (2010). Using of silica particles as porogen for preparation of macroporous chitosan macrospheres suitable for enzyme immobilization. *Kinetics and Catalysis*, *51*, 771–775.

Sun, W., Qin, P., Gao, H., Li, G., & Jiao, K. (2010). Electrochemical DNA biosensor based on chitosan/nano-V_2O_5/MWCNTs composite film modified carbon ionic liquid electrode and its application to the LAMP product of *Yersinia enterocolitica* gene sequence. *Biosensors and Bioelectronics*, *25*, 1264–1270.

Talbert, J., & Hotchkiss, J. (2012). Chitosan-tethered microspheres for lactase immobilization. *Journal of Molecular Catalysis B: Enzymatic*, *78*, 78–84.

Tortajada, M., Ramon, D., Beltrand, D., & Amoros, P. (2005). Hierarchical bimodal porous silica and organosilica for enzyme immobilization. *Journal of Material Chemistry*, *15*, 3859–3868.

Trpathi, S., Goyal, R., Kumar, P., & Gupta, K. (2012). Linear polyethylenimine-graft-chitosan copolymers as efficient DNA/siRNA delivery vectors in vitro and in vivo. *Nanomedicine: Nanotechnology, Biology, and Medicine*, *8*, 337–345.

Zhang, J., Yuan, Y., Shen, J., & Lin, S. (2003). Synthesis and characterization of chitosan grafted poly(N,N-dimethyl-N-methacryloxyethyl-N-(3-sulfopropyl) ammonium) initiated by ceric (IV) ion. *European Polymer Journal*, *39*, 847–850.

Zhang, W., Wang, N., Zhou, Y., He, T., & Yu, X. (2012). Enhancement of activity and stability of lipase by microemulsion-based organogels (MBGs) immobilization and application for synthesis of arylethyl acetate. *Journal of Molecular Catalysis B: Enzymatic*, *78*, 65–71.

Zhang, Y., Zhang, Y., Wang, H., Yan, B., Shen, G., & Yu, R. (2009). An enzyme immobilization platform for biosensor designs of direct electrochemistry using flower-like ZnO crystals and nano-sized gold particles. *Journal of Electroanalytical Chemistry*, *627*, 9–14.